

D.V. Bugg,
Queen Mary, University of London, London E1 4NS, UK

Abstract

The threshold $\bar{p}p$ peak in BES data for $J/\Psi \rightarrow \gamma\bar{p}p$ may be fitted as a cusp. It arises from the well known threshold peak in $\bar{p}p$ elastic scattering due to annihilation. Several similar examples are discussed. The PS185 data for $\bar{p}p \rightarrow \bar{\Lambda}\Lambda$ require an almost identical cusp at the $\bar{\Lambda}\Lambda$ threshold. There is likewise a cusp at the ΣN threshold in $K^-d \rightarrow \pi^-(\Lambda p)$. Similar cusps are likely to arise at thresholds for all 2-body de-excitation processes, providing the interaction is attractive; likely examples are $\Lambda\bar{p}$, $\Sigma\bar{p}$, and $\bar{K}\Lambda$. The narrow peak observed by Belle at 3872 MeV in $\pi^+\pi^-J/\Psi$ may be a $J^{PC} = 1^{++}$ cusp due to the $D\bar{D}^*$ threshold. The narrow $\Xi^*(1862)$ observed by NA49 may be due to a threshold cusp in $\Sigma(1385)\bar{K}$ coupled to $\Xi\pi$ and $\Sigma\bar{K}$. The relation of cusps to known resonances such as $f_0(980)$ is discussed.

Wigner pointed out that a cusp appears in the cross section for any process at the threshold where a coupled channel opens [1]. Such cusps were studied in the 1958-61 era by Baz' and Okun [2], Nauenberg and Pais [3] and others. Törnqvist has emphasised the importance of cusps in meson-meson scattering and their relation to resonances [4].

Several narrow peaks attributed to resonances may in fact be cusp effects. The cusp has a different structure to a resonance: the behaviour of the real part of the amplitude is quite different. Under some circumstances, a threshold can induce or capture a resonance. The conditions under which a resonance is likely to be trapped are discussed using $f_0(980)$ as an example.

The BES collaboration reports a threshold $\bar{p}p$ peak in $J/\Psi \rightarrow \gamma\bar{p}p$ [5], and fits it as a narrow resonance just below the $\bar{p}p$ threshold. Datta and O'Donnell conjecture a narrow quasi-bound state of $\bar{p}p$ [6]. The Belle collaboration has also reported low mass $\bar{p}p$ peaks in $B^+ \rightarrow K^+\bar{p}p$ [7] and $\bar{B}^0 \rightarrow D^0\bar{p}p$ [8].

In view of the very large number of open channels known in $\bar{p}p$ annihilation at rest, a narrow resonance is surprising. Why should such a resonance be narrow compared to conventional meson widths of ~ 250 MeV?

There are threshold peaks in the $\bar{p}p$ total cross section [9] and annihilation cross section [10,11]; both rise continuously towards threshold and may be parametrised as $A + B/k$, where k is centre of mass momentum. The

B/k term follows the familiar ‘ $1/v$ law’ of thermal neutron physics and is symptomatic of absorption from the $\bar{p}p$ channel into other open channels [12].

The process $J/\Psi \rightarrow \gamma \bar{p}p$ will be discussed following Watson’s treatment of final-state interactions [13]. The production process is considered in terms of two vertices. The first produces γX ; most details of the production mechanism will be neglected, therefore absolute cross sections cannot be predicted. Attention will be focussed on a second vertex where all channels having the quantum numbers of X participate in a final-state interaction. From this second vertex, the $\bar{p}p$ channel is one of the emergent channels. If the second vertex is resonant, one arrives at the conventional Isobar Model. Rescattering between the spectator photon and decay products of X is neglected.

The final-state interaction may also be non-resonant: a familiar example is $\pi^- d \rightarrow \gamma(nn)$, which provides one of the best measurements of the nn scattering length. Suppose the amplitude f_S for $\bar{p}p$ elastic scattering is written in the N/D form, where $N(s)$ has only left hand cuts and $D(s)$ has only right-hand cuts. The content of Watson’s theorem is that $D(s)$ is the same for all channels in which $\bar{p}p$ appears. The structure in BES data should be the same as in $\bar{p}p$ elastic scattering.

The data will be fitted using a scattering length approximation $k \cot \delta = 1/a$, where a is complex. If the S-wave amplitude is written as $f_S = (e^{2i\delta} - 1)/2ik$, simple K-matrix algebra gives

$$f_S = \frac{a}{1 - iak} = \frac{a + i|a|^2 k}{1 + 2k \operatorname{Im} a + k^2 |a|^2}, \quad (1)$$

$$|f_S|^2 = \frac{|a|^2}{1 + 2k \operatorname{Im} a + k^2 |a|^2}. \quad (2)$$

Eqn. (2) expresses the enhancement factor for a non-resonant final-state interaction. The k -dependent terms are due to unitarity and guarantee that f_S obeys the unitarity limit for large k . The total cross section $\sigma_{tot} = 4\pi \operatorname{Im} f_S/k$, follows the $1/v$ law, as does the inelastic cross section.

There is a step in $\operatorname{Im} f_S$ at threshold (since it vanishes below threshold). The real part of the amplitude is given by a dispersion relation:

$$\operatorname{Re} f_S(s) = \frac{1}{\pi} \operatorname{P} \int \frac{\operatorname{Im} f_S(s') ds'}{s' - s}. \quad (3)$$

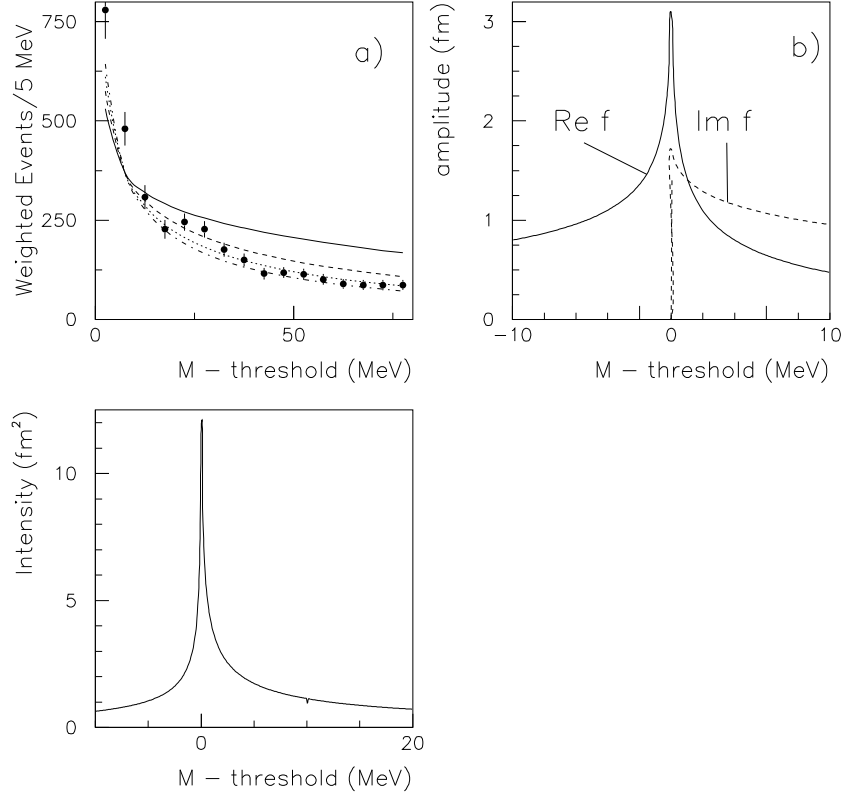


Figure 1: (a) The $\bar{p}p$ mass spectrum observed by BES, after dividing out S-wave phase space. Curves show fits to a scattering length approximation with $\text{Im } a = 0.6$ fm (full curve), 1.2 fm (dashed), 1.8 fm (dotted) and 2.4 fm (chain), including the dispersive corrections to $\text{Re } f_S$; (b) real and imaginary parts of f_S within 10 MeV of threshold; (c) $|f_S|^2$, including its analytic continuation below threshold.

If $\text{Im } f_S$ were strictly constant, $\text{Re } f_S$ would be logarithmically divergent:

$$\text{Re } f_S = \frac{\text{Im } a}{\pi} \ln \left(\frac{4M^2 - s_0}{|4M^2 - s|} \right). \quad (4)$$

The full eqns. (1) and (3) give a convergent but similar peak in $\text{Re } f_S$ at threshold, as illustrated in Fig. 1(b). The peak is positive both below and above threshold. The dispersive peak in $\text{Re } f_S$ represents an effective attraction, which can lock a resonance at or close to the threshold.

Fig. 1(a) shows BES data, after dividing out the S-wave phase space factor, as in their Fig. 3(b), from which the data points are taken. Curves show results from eqn. (2) for several values of $\text{Im } a$. The real part of the amplitude is included from eqn. (3) using a subtraction at $k = 110$ MeV/c, where Coulomb interference data give $\rho = \text{Re } f(0)/\text{Im } f(0) \sim 0$ [14]. The best fit requires $\text{Im } a \simeq 1.8$ fm (dashed curve). Fig. 1(b) is plotted with this value. However, this number is not well determined because (i) there could well be an effective range term in f_S , (ii) there is the possibility of some P-wave contributions to BES data at the higher masses.

Production of the $\bar{p}p \ ^1S_0$ final state in $J/\Psi \rightarrow \gamma \bar{p}p$ requires orbital angular momentum $L = 1$ at the production vertex. A factor E_γ^3 is included into the production cross section, since the $c\bar{c}$ interaction is ‘pointlike’; this factor enhances the lowest $\bar{p}p$ masses slightly. The cross section is also enhanced by the Coulomb attraction near threshold by a factor $(1 - e^{-X})/X$, where $X = \pi\alpha/\beta$ and $\beta^2 = 1 - 4M^2/s$ [15]; M is nucleon mass. This factor affects only the first two points significantly. The lowest point is enhanced by 19% and the highest by 4.4%, so Coulomb attraction does not account for the peak.

The $\bar{p}p$ annihilation cross section is close to the unitarity limit [16]. The cross section for $\bar{p}p \rightarrow \bar{n}n$ is very small. The amplitude for this process depends on $f_S(I = 1) - f_S(I = 0)$ and therefore requires an accurate cancellation between the imaginary parts of amplitudes for the two isospins. If the threshold peak were due to a narrow resonance, this would require two $I = 1$ and $I = 0$ resonances accurately degenerate in mass, width and coupling strength. Such a triple coincidence is implausible, since attractive forces from meson exchanges are likely to be significantly different for the two isospins. This is a first argument against a resonance interpretation.

Consider next $\bar{p}p \rightarrow \bar{\Lambda}\Lambda$. The PS185 collaboration has measured cross sections at fine steps of \bar{p} momentum very close to threshold [17]. A full

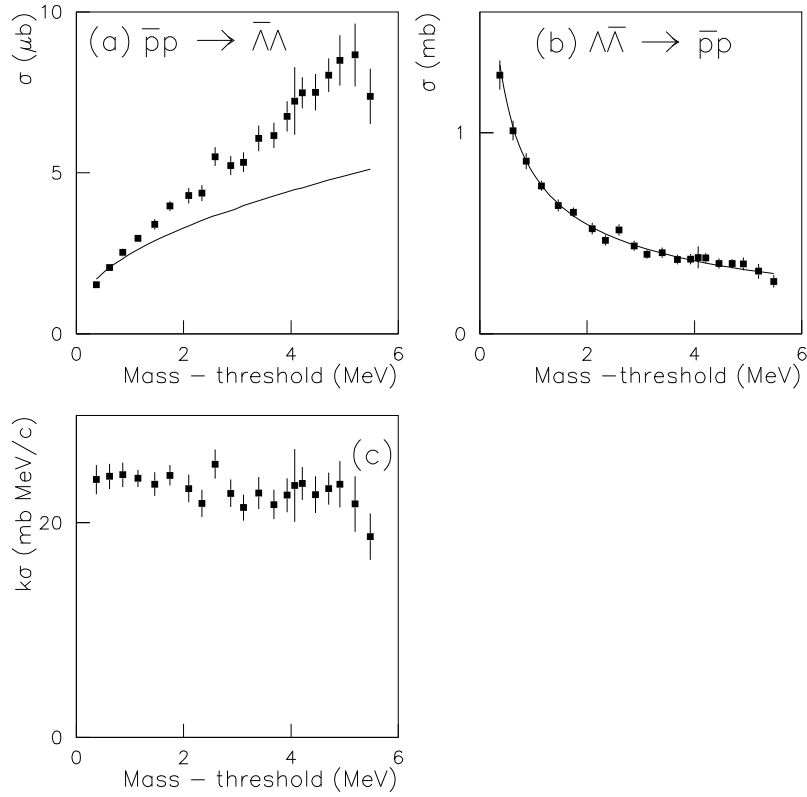


Figure 2: (a) PS 185 integrated cross sections for $\bar{p}p \rightarrow \bar{\Lambda}\Lambda$; the curve shows the S-wave cross section from a phase shift analysis; (b) the corresponding cross section for $\bar{\Lambda}\Lambda \rightarrow \bar{p}p$, after subtracting P-wave cross sections; the curve is a fit using eqns. (2) and (3); (c) $\sigma(\bar{\Lambda}\Lambda \rightarrow \bar{p}p) \times k$ v. excitation energy after subtracting P-waves.

partial wave analysis, including extensive spin dependent data, is reported elsewhere [18]. The data points of Fig. 2(a) show integrated cross sections. The curve shows the cross section fitted to the $\bar{\Lambda}\Lambda$ S-wave; the difference from data is due to $\bar{\Lambda}\Lambda$ P-waves, which are well determined by polarisation data and the forward-backward asymmetry in $d\sigma/d\Omega$. The P-waves are surprisingly large. A possible reason, proposed by PS185, is that P-waves are highly peripheral, and do not suffer from absorption into other channels; in the mass range shown in Fig. 2, $k < 85$ MeV/c corresponding to an impact parameter > 2 fm.

Using detailed balance, the cross section for the inverse process may be derived:

$$\sigma(\bar{\Lambda}\Lambda \rightarrow \bar{p}p) = \frac{k_p^2}{k_\Lambda^2} \sigma(\bar{p}p \rightarrow \bar{\Lambda}\Lambda), \quad (5)$$

where k_p and k_Λ are centre of mass momenta of p and $\bar{\Lambda}$. Fig. 2(b) shows resulting cross sections after subtracting P-wave contributions. There is a definite cusp at the $\bar{\Lambda}\Lambda$ threshold. It has not been reported before. Fig. 2(c) shows that this cross section fits a $1/k$ dependence. The peak of Fig. 2(b) appears narrower than the $\bar{p}p$ peak of Fig. 1(a) because one is looking at different parts of the $1/v$ curve, but they can both be fitted with an identical value of $\text{Im } a$. The cross section of Fig. 2(b) reaches 1 mb at 0.5 MeV excitation energy. If the $\bar{\Lambda}\Lambda$ annihilation cross section reaches its unitarity limit (> 500 mb at the same energy), $\bar{\Lambda}\Lambda \rightarrow \bar{p}p$ can only be one of a large number of open channels.

A third example of a cusp is in $K^-d \rightarrow \pi^- \Lambda p$, where a peak is observed [19,20] in the Λp mass spectrum at the ΣN threshold. My fit with a cusp is shown in Fig. 3, using the weighted mean of data from Refs. [19] and [20]. Separate cusps are fitted to $\Sigma^0 p$ and $\Sigma^+ n$, weighted in the ratio 2: 1 of Clebsch-Gordan coefficients for $I = \frac{1}{2}$ (Λp). The optimum fit requires shifting experimental data upwards by 1 MeV, within their errors.

The data have also been fitted by Dosch and Stamatescu [21], who conclude that there is a 3S_1 pole. Earlier, Nagels, Rijken and de Swart [22] fitted hyperon-nucleon scattering data at low energies and required a $\Sigma^+ n$ pole at 2131.77 - i2.39 MeV, very close to the Σn threshold. Its width is so small that it is difficult to separate from a cusp effect with existing data.

Next, the Belle collaboration has presented evidence for a very narrow $\pi^+\pi^- J/\Psi$ peak at 3872 MeV in $B^\pm \rightarrow K^\pm(\pi^+\pi^- J/\Psi)$ [23]. This mass is 0.8

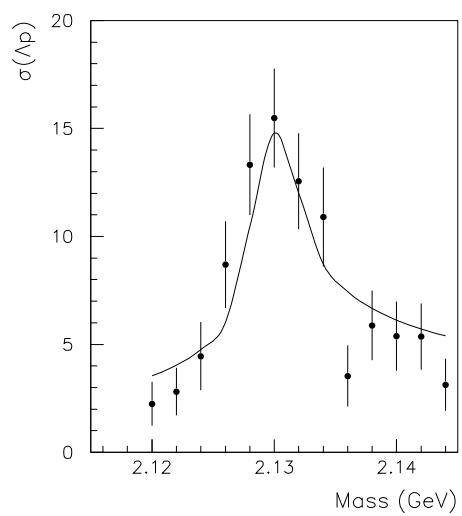


Figure 3: The Λp mass spectrum from the weighted mean of data from Refs. [18] and [19]; the curve shows the fit to a cusp. The vertical scale is unnormalised.

MeV above the $D^0\bar{D}^{0*}$ threshold and 7 MeV below that for $D^\pm\bar{D}^{\mp*}$. The peak could well be due to an S-wave cusp expected at the mean threshold of 3875 MeV.

Suppose $D\bar{D}^*$ final states are produced randomly in the production process. Those close to threshold follow a $1/v$ cross section for de-excitation to open channels. [A proviso is that the $\bar{D}D^*$ interaction is attractive near threshold; if the real part of the interaction is repulsive, the wave function at low momentum may be shielded from short range annihilation.] There are many open channels: $J/\Psi\rho$, $[\eta_c(\pi\pi)_S]_{L=1}$, $[\chi_{c0}\pi]_{L=1}$, $[\chi_{c1}\pi]_{L=1}$ and $\chi_{c1}(\pi\pi)_S$, where $(\pi\pi)_S$ denotes the $\pi\pi$ S-wave. The observed cross section in a final state such as $J/\Psi\rho$ will be given by $D\bar{D}^*$ phase space multiplied into the de-excitation cross section. The $1/k$ dependence of the cross section is almost cancelled by the k/\sqrt{s} dependence of the phase space; the variation of $J/\Psi\rho$ phase space over the narrow region being considered is also negligible. Neglecting these two factors, the result is given by eqn. (2).

Fig. 1(c) illustrates the corresponding result for any channel fed by $p\bar{p}$. The peak comes from the dispersive effect in the real part at threshold. If the final state is fed entirely by $\bar{p}p$ annihilation, the peak will be cut off sharply below threshold. However, it is also possible for the final states to be produced via other mechanisms. These will have precisely the same s -dependence, since the final state ‘knows’ about the threshold through analyticity. The dispersive peak marks the opening of the 2-body channel, both in $\bar{p}p$ and in $D\bar{D}^*$.

Further threshold cusps may arise in all annihilation channels involving narrow particles, providing the interaction is attractive, so that the annihilation is not suppressed. Possible examples are $D\bar{D}$ (due to decay to $J/\Psi\rho$ and $\chi_{c0}(\pi\pi)_S$), $D^*\bar{D}^*$ ($J^P = 2^+, 1^+$ or 0^+ with many open channels), $\Xi\bar{p}$, $\Sigma\bar{p}$, $\Lambda\bar{p}$ and so on.

Example 5 is the narrow peak at 1862 MeV observed by the NA49 collaboration in $\Xi^-\pi^-$, $\Xi^-\pi^+$ and their charge conjugates [24]. It requires exotic quantum numbers $I = 3/2$ and has been proposed as a pentaquark. The $\Sigma(1385)\bar{K}$ threshold lies slightly higher. The $\Sigma(1385)\bar{K}$ pair can de-excite to $\Sigma\bar{K}$, $\Xi\pi$ and $\Xi^*(1530)\pi$. An illustration of the process is shown in Fig. 4(a). All these processes are likely to have $1/v$ cross sections near the $\Sigma(1385)\bar{K}$ threshold.

Using eqn. (2), it is a simple matter to fold the energy dependence of the de-excitation process $\Sigma(1385)\bar{K} \rightarrow \Xi\pi$ with the line-shape of $\Sigma(1385)$.

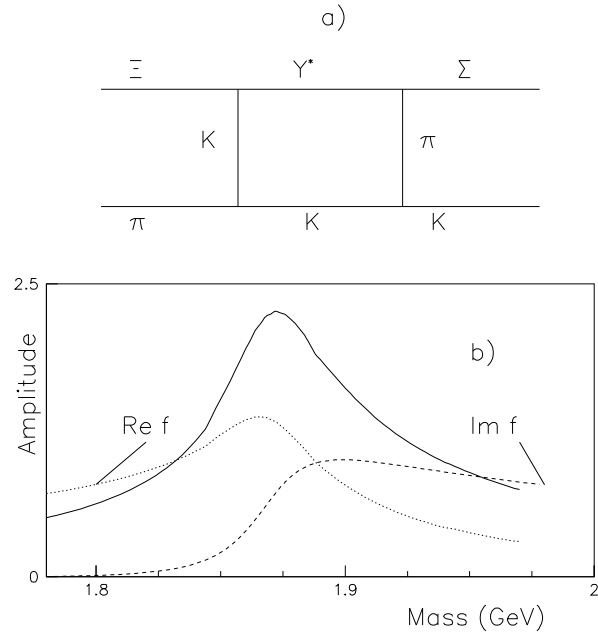


Figure 4: (a) The Graph for de-excitation of $\Sigma(1385)\bar{K}$ to $\Xi\pi$ and ΣK ; (b) Real (dotted) and Imaginary (dashed) parts of the $\Sigma(1385)\bar{K}$ elastic amplitude and its intensity (full curve).

The calculation assumes a $\Sigma(1385)\bar{K}$ scattering length of 1.8 fm, as for $\bar{p}p$; however, there is very little sensitivity to this value, except for the absolute normalisation. The calculation uses a P-wave line-shape of $\Sigma(1385)$ with a centrifugal barrier radius of 0.8 fm. It also includes mass differences between charge states with a weighting for charges taken from the NA49 data. Fig. 4(b) shows Real and Imaginary parts of the $\Sigma(1385)\bar{K}$ elastic scattering amplitude. The imaginary part rises like a Fermi function due to the width of $\Sigma(1385)$. The intensity is shown in Fig. 4(b) by the full curve. It gives rise to a peak in de-excitation channels, e.g. $\Xi^-\pi^-$, centred at 1872 MeV. The NA49 collaboration quotes a mass of 1862 ± 2 MeV for $\Xi^-\pi^-$ and 1864 ± 5 MeV for $\Xi^-\pi^+$. So there remains a discrepancy of $\sim 9 \pm 3$ MeV with the predicted mass. This discrepancy could arise from interference with background amplitudes. The width quote by NA49 also appears to be smaller: < 18 MeV.

There is a useful and well documented analogue in heavy ion elastic scattering at the Coulomb barrier, observed in a wide variety of examples throughout the nuclear periodic table. The topic is reviewed by Satchler [25]. Real and imaginary parts of the optical potential are derived from accurate experimental data. The imaginary part of the potential rises swiftly as the Coulomb barrier is overcome and inelastic channels open. This is analogous to the dashed curve of Fig. 4(c). The real part of the potential peaks at the centre of the leading edge, like the peak in $\text{Re } f_S$. Satchler's Fig. 2.2 for $^{16}\text{O} + ^{208}\text{Pb}$ elastic scattering is very similar to Fig. 4(b).

A final example of a cusp is in $\pi d \rightarrow NN$ below 10 MeV [26]. In this case, it is well known that there is no 3P_1 NN resonance at this threshold. In fact, the NN 3P_1 phase shift is repulsive.

In all these cases, cusps may account for the data, but there is also the possibility of a resonance interpretation. To understand whether a resonance is likely, it is instructive to consider $f_0(980)$ as an example. This resonance is fitted with the Flatté form:

$$f_S = 1/[M^2 - s - m(s) - iM(g_\pi^2 \rho_{\pi\pi}(s) + g_K^2 \rho_{K\bar{K}}(s))], \quad (6)$$

$$m(s) = \frac{M^2 - s}{\pi} \int \frac{M\Gamma_{\text{tot}}(s') ds'}{(M^2 - s')(s' - s)}, \quad (7)$$

where g are coupling constants and ρ is 2-body phase space $2k/\sqrt{s}$. Parameters will be taken from the latest BES data on $J/\Psi \rightarrow \phi\pi^+\pi^-$ and ϕK^+K^- ,

where the $f_0(980)$ is particularly well determined in both $\pi\pi$ and KK decay modes [27].

The Argand diagram for the $\pi\pi \rightarrow \pi\pi$ amplitude is shown on Fig. 5(a). The $K\bar{K}$ threshold opens at the point T , creating a cusp. The amplitude is

$$\begin{aligned} f(\pi\pi \rightarrow \pi\pi) &= \frac{1}{k_\pi} \frac{2g_\pi^2 k_\pi / \sqrt{s}}{M^2 - s - m(s) - 2iM(g_\pi^2 k_\pi + g_K^2 k_K) / \sqrt{s}} \\ &= \frac{2g_\pi^2 / \sqrt{s}}{M^2 - s - m(s) - 2iM(g_\pi^2 k_\pi + g_K^2 k_K) / \sqrt{s}}. \end{aligned} \quad (8)$$

Amplitudes for $K\bar{K} \rightarrow K\bar{K}$ and $K\bar{K} \rightarrow \pi\pi$ are obtained by replacing g_π^2 by g_K^2 or $g_\pi g_K$; note that all three amplitudes share the same dependence on s , i.e. the same denominator $D(s)$.

The dispersive contribution to $\text{Re} f$ from eqns. (2) and (3) is shown in Fig. 5(b), taking $\text{Im} a = 0.87$ fm from the Flatté fit to data. It spreads over a wider mass range than for $\bar{p}p$, Fig. 1(b), because $\text{Im} a$ is smaller. The dotted curve on Fig. 5(b) shows the actual line-shape of the Flatté formula. There is quite a good overlap between the dispersive component of $\text{Re} f_s$ and the line-shape of the resonance. One must remember that there are also attractive forces due to meson exchanges [28,29] and/or attraction at the quark level. These add coherently to the dispersive contribution to $\text{Re} f_s$ and play a role in deciding whether or not a resonance appears. Janssen et al. remark that the attraction arising from the $K\bar{K}$ threshold is important in their model of $f_0(980)$.

For a resonance to develop, the attraction must overcome zero-point energy, which is large if the wave function is tightly constrained to small r . A segment of the line-shape with binding energy B beneath the $K\bar{K}$ threshold has a radial wave function $\propto e^{-\alpha r}/r$, where $\alpha = 1/\sqrt{M_K B}$ and M_K is the kaon mass. The smaller the value of B , the lower is the zero-point energy. The part of the wave function outside the short-range attraction contributes negatively to zero-point energy; the wave function is exponentially damped rather than oscillatory.

The ideal circumstance for a resonance locked to the threshold arises when a single channel (denoted 1) above threshold is coupled weakly to one other channel (2) below threshold, as for $f_0(980)$ and $a_0(980)$. If wave function leaks away into many other channels, (i) the resonance acquires a width $g_i^2 \rho_i(s)$ through coupling to each such channel i , (ii) $\text{Re} f_s(s)$ arising from channel 1 is weakened because wave function is lost from that channel.

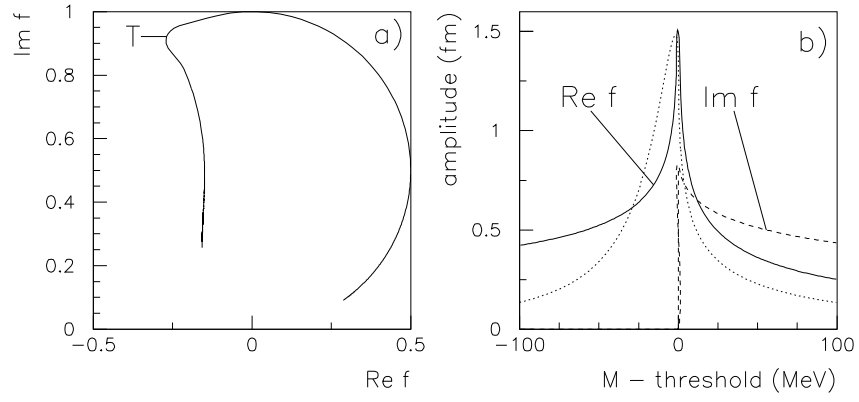


Figure 5: (a) The Argand diagram for $f_0(980)$; T marks the $K\bar{K}$ threshold; (b) $\text{Re } f$ (full curve), $\text{Im } f$ (dashed) from eqns. (2) and (3) compared with the actual line-shape of $f_0(980)$ (dotted).

If one views the $\bar{p}p$ and $\bar{\Lambda}\Lambda$ peaks in this light, resonances are unlikely. For $\Sigma n \rightarrow \Lambda p$, the data lie close to the unitarity limit, so again the cusp interpretation appears more likely. Nagels et al. [22] circumvent this by putting their bound state so close to threshold that most of the wave function lies far outside the range of nuclear interactions.

The branching fraction measured for $J/\Psi \rightarrow \gamma \bar{p}p$ is 7×10^{-5} [5]. However, there are much larger branching fractions for $J/\Psi \rightarrow \gamma X$ with X having the same quantum numbers $J^{PC} = 0^{-+}$, $I = 0$. These channels are $\rho\rho$, $\omega\omega$, $K^*\bar{K}^*$, $\eta\pi\pi$ and $K\bar{K}\pi$; their combined branching fraction is $(1.9 \pm 0.3) \times 10^{-2}$ from Fig. 2 of Bugg, Dong and Zou [30]. This is a second argument against a resonance. The BES collaboration sees no threshold $\bar{p}p$ peak in the final state $\pi^0 \bar{p}p$. This final state has a branching fraction 10^{-3} , much larger than $\gamma \bar{p}p$. It is likely to be dominated by $N^*\bar{N}$ and $\Delta\bar{N}$ channels; their angular momenta have only small overlap (Racah coefficients) with $N\bar{N}$ S-waves.

In summary, cusps are capable of explaining in a simple way peaks observed at many thresholds. These cusps are a direct consequence of decay to open channels. The cusp is driven by the peaking of the S-wave de-excitation cross section due to the $1/v$ law. The singularity at a cusp is of the form $a/(1 - iak)$ and has a real part different from a resonance. A resonance is to be expected only under restrictive circumstances such as those for $f_0(980)$, where there is a single weak open channel.

While this work was being written up, a related paper has appeared from Kerbikov, Stavinsky and Fedotov [31]. They also attribute the narrow structure in $\bar{p}p$ to a cusp and fit it with the scattering length approximation; they do not however consider the dispersive contribution to $\text{Re}f_s$.

I am grateful to Dr. T. Johansson for tables of PS 185 data and to Prof. J. de Swart for comments on hyperon-nucleon scattering.

References

- [1] E.P. Wigner, Phys. Rev. 73 (1948) 1002.
- [2] A.N. Baz' and L.B. Okun, J. Exptl. Theor. Phys. 35 (1958) 757; [Translation: Soviet Phys. -JETP 8 (1959) 526].
- [3] M. Nauenberg and A. Pais, Phys. Rev. 123 (1961) 1058 and 126 (1962) 360.

- [4] N.A. Törnqvist, Z. Phys. C68 (1995) 647.
- [5] J.Z. Bai et al., Phys. Rev. Lett. 91 (2003) 022001-1.
- [6] A. Datta and P.J. O'Donnell, Phys. Lett. B567 (2003) 273.
- [7] K. Abe et al., Phys. Rev. Lett. 88 (2002) 181803.
- [8] K. Abe et al., Phys. Rev. Lett. 89 (2002) 151802.
- [9] D.V. Bugg et al., Phys. Lett. B194 (1987) 563.
- [10] A. Bertin et al., Phys. Lett. B369 (1996) 77.
- [11] A. Zenoni et al., Phys. Lett. B461 (1999) 405.
- [12] L.D. Landau and E.M. Lifshitz, *Quantum Mechanics*, Pergamon Press, London, 1959, pp 438-440.
- [13] K.M. Watson, Phys. Rev. 88 (1952) 1163.
- [14] L. Linssen et al., Nucl. Phys. A469 (1987) 726.
- [15] A.D. Sakharov, ZhETF 18 (1948) 631.
- [16] E. Klempt, F. Bradamante, A. Martin and J-M. Richard, Phys. Rep. 368 (2002) 119.
- [17] P.D. Barnes et al., Phys. Rev. C62 (2000) 055203 and references given there.
- [18] D.V. Bugg, *Partial Wave Analysis of $\bar{p}p \rightarrow \bar{\Lambda}\Lambda$* , submitted to Euro. Phys. C.
- [19] D. Eastwood et al., Phys. Rev. D3 (1971) 2603.
- [20] O. Braun et al., Nucl. Phys. B124 (1977) 45.
- [21] H.G. Dosch and I.O. Stamatescu, Z. Phys. C3 (1980) 249.
- [22] M.M. Nagels, T.A. Rijken and J.J. de Swart, Phys. Rev. D20 (1979) 1633.

- [23] S.-K.Choi et al., Phys. Rev. Lett. 91 (2003) 262001.
- [24] C. Alt et al., Phys. Rev. Lett. 92 (2004) 042003.
- [25] G.R. Satchler, Phys. Rep. 199 (1991) 148.
- [26] J. Spuller and D.F. Measday, Phys. Rev. D12 (1975) 3550.
- [27] L.Y. Dong (private communication).
- [28] D. Lohse, J.W. Durso, K. Holinde and J. Speth, Phys. Lett. B234 (1990) 235.
- [29] G. Janssen, B.C. Pearce, K. Holinde and J. Speth, Phys. Rev. D52 (1995) 2690.
- [30] D.V. Bugg, L.Y. Dong, and B.S. Zou, Phys. Lett. B458 (1999) 511.
- [31] B. Kerbikov, A. Stavinsky and V. Fedotov, hep-ph/0402054.